13th HEAD Meeting – Monterey, CA, USA, 2013 April 7–11

Exposing the symbiosis of 3A 1954+319

Katja Pottschmidt[1,2], Diana M. Marcu[1,2], Natalie Hell[3,4], Felix Fürst[5], Ivica Miškovičová[3], Sebastian Müller[3], Victoria Grinberg[3], Robin H.D. Corbet[1,2], Jörn Wilms[3]

[1]CRESST/NASA-GSFC, Greenbelt, MD, USA, [2]UMBC, Baltimore, MD, USA, [3]Dr. Karl Remeis-Observatory/ECAP/FAU, Bamberg, Germany
[4]Lawrence Livermore Laboratory, Livermore, CA, USA, [5]SRL, Caltech, Pasadena, CA, USA

E-mail: katja@milkyway.gsfc.nasa.gov

Abstract

Symbiotic X-ray Binaries (SyXB) are a rare class (~8 known members) of Low Mass X-ray Binaries (LMXB), in which a compact object accretes material from an evolved **M-type giant companion**. The SyXB and **accreting pulsar** 3A 1954+319 is further exceptional since it has the longest pulse period known for an X-ray binary. It undergoes rapid changes, which we found span a range of 5.0–5.8 h over the interval 2005–2012 monitored with *Swift*-BAT, probably an indication of the expected strong interaction with the dense M-giant wind.

We present an analysis of a ***Chandra*** observation performed on 2010, December 26, and an ***RXTE*** observation performed on 2011, January 10–11. The *Swift*-BAT context shows that during both observations the source was in a state of comparatively stable and low hard X-ray flux. We discuss the broad band "baseline" spectrum and compare it to the two earlier X-ray broad band studies described in the literature. Strong flaring activity on timescales of hundreds to thousands of seconds is observed and studied in the light of a possible accretion shock interpretation.

3A 1954+319: A Rare Type of X-ray Binary

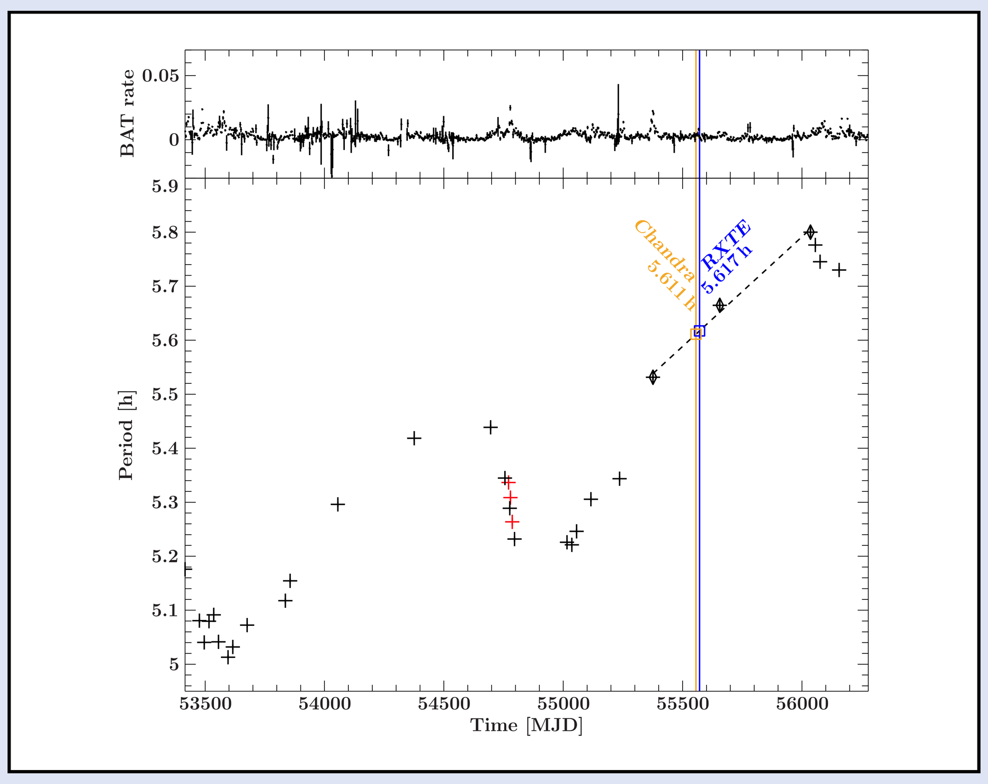

FIGURE 1: Top: *Swift*-BAT 15–50 keV lightcurve [counts s^{-1} cm^{-2}]. Bottom: BAT pulse period evolution with estimated values for the *Chandra* & *RXTE* observations. Red crosses: *INTEGRAL* data.

3A 1954+319 was detected as a highly variable X-ray source in surveys by *Uhuru* and *Ariel V* (Forman et al., 1978; Warwick et al., 1981). Masetti et al. (2006) identified the M-type giant companion, placing the source into a small group of **LMXB wind accretors** (Nespoli et al., 2010). The orbital period is not known.

Corbet et al. discovered a ~5 h period in the 2005 BAT data and interpreted it as the neutron star's pulse period (Corbet et al., 2006, 2008). In 2008 the source showed renewed activity, observed as part of the *INTEGRAL* Cygnus Region Key Program. In addition to a strong spin-up of -1.8×10^{-4} h h^{-1} (red crosses in Fig. 1) we found that the ~5.3 h pulse was directly visible in the > 20 keV *INTEGRAL* lightcurves (Marcu et al., 2011).

In order to **check for signatures of the dense stellar wind** we performed quasi-simultaneous *Chandra* grating and *RXTE* observations on 2010/12/26 and 2011/01/10, respectively. As can be seen in Fig. 1 they happened during a long spin-down trend that reversed only recently. According to BAT the pulse period had increased to ~5.6 h (~20 ks) and the > 15 keV source flux was ~10–20 mCrab showing comparatively little variability on timescales of weeks.

Chandra-HETG Spectrum

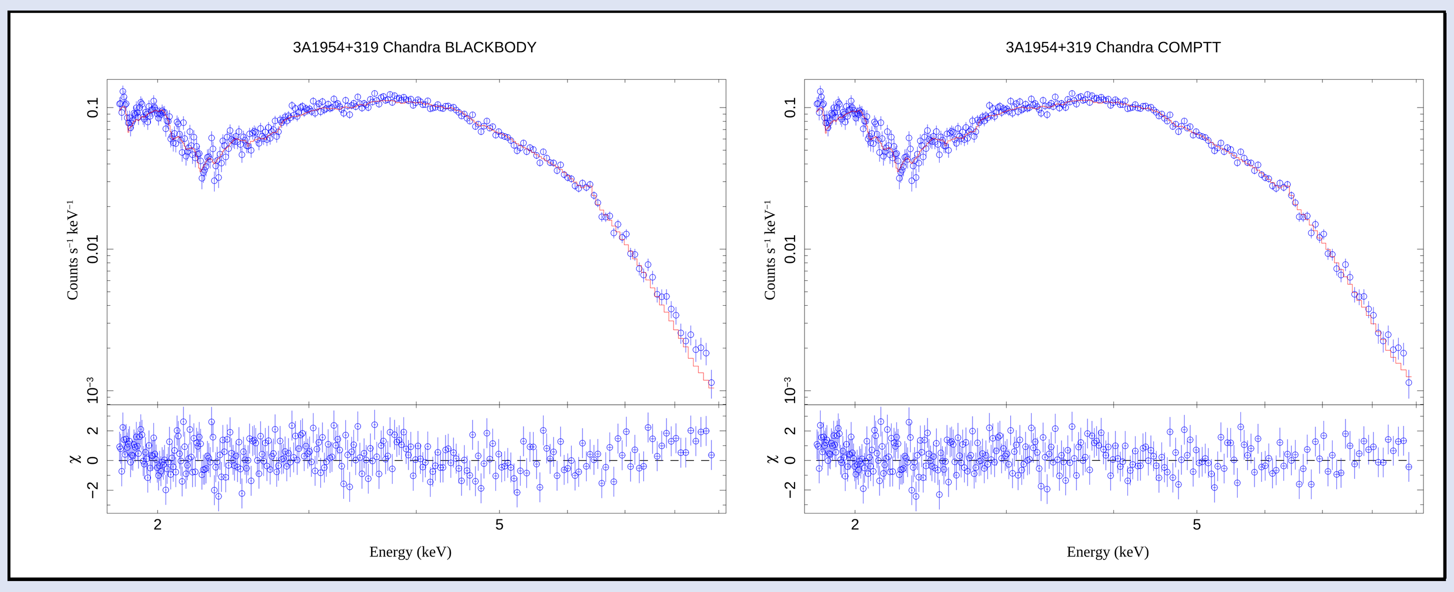

FIGURE 2: *Chandra* MEG & HEG 1st order spectrum with bestfit and residuals for two different models.
Left: `tbnew×(bbody+gauss[Fe])`. Right: `tbnew×(comptt+gauss[Fe])`.

We extracted the 1st order MEG and HEG grating spectra (~37 ks each), rebinned them (SNR > 4.5, no. of channels > 16), and modeled them jointly in the energy range 1.8–9.0 keV. Different versions of cutoff power law models (`cutoffpl`, `highecut`, `fdcut`) only resulted in good fits for unphysical parameters ($\Gamma < 0$). Acceptable fits of comparable quality were obtained for both the `diskbb` (χ^2_{red}/dof=1.05/91; Fig. 2, left) and the `comptt` (χ^2_{red}/dof=1.04/89; Fig. 2, right) continuum.

`diskbb`: $N_{\mathrm{H}} = 3.3(1) \times 10^{22}\,\mathrm{cm}^{-2}$, $kT_0 = 1.64(3)\,\mathrm{keV}$, $A_{\mathrm{Fe}} = 1.1(7) \times 10^{-4}\,\mathrm{ph\,cm^{-2}\,s^{-1}}$
`comptt`: $N_{\mathrm{H}} = 2.0(2) \times 10^{22}\,\mathrm{cm}^{-2}$, $kT_0 = 1.2(1)\,\mathrm{keV}$, $A_{\mathrm{Fe}} = 1.1(7) \times 10^{-4}\,\mathrm{ph\,cm^{-2}\,s^{-1}}$,
$kT_{\mathrm{e}} > 2\,\mathrm{keV}$, $\tau < 7$ (only Compton-y is constrained)

Apart from the known Fe Kα line at 6.4 keV we do not detect any emission or absorption lines. For the *Chandra* data alone no complex absorption / hot plasma emission (`pcfabs, windabs, mekal;` Masetti et al., 2007) or low temperature black body (Mattana et al., 2006) is required.

RXTE-PCA Spectrum

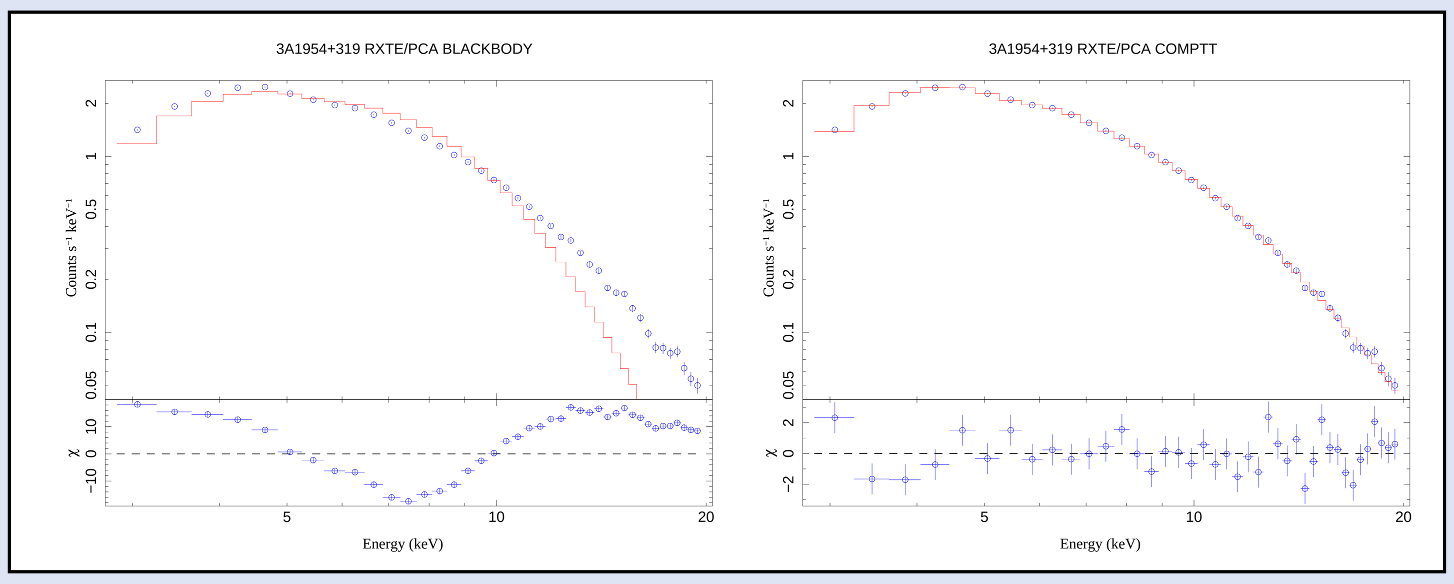

FIGURE 3: *RXTE* PCA PCU2 spectrum with bestfit and residuals for two different models.
Left: `tbnew×(bbody+gauss[Fe])`. Right: `tbnew×(comptt+gauss[Fe])`.

We extracted the PCA PCU2 spectrum (~35 ks) using the `standard2f` binning and modeled it in the energy range 2.5–20 keV. Not unexpectedly the `bbody` continuum does not provide a good description into the higher energy range (Fig. 3, left). Different versions of cutoff power law models, e.g., `cutoffpl` (χ^2_{red}/dof=1.43/35), as well as `comptt` (χ^2_{red}/dof=1.46/34; Fig. 3, right) provide acceptable fits of comparable quality. **`diskbb`**: No good fit.

`cutoffpl`: $N_{\mathrm{H}} = 4.5^{+0.4}_{-0.8} \times 10^{22}\,\mathrm{cm}^{-2}$, $A_{\mathrm{Fe}} = 0.8(3) \times 10^{-4}\,\mathrm{ph\,cm^{-2}\,s^{-1}}$,
$E_{\mathrm{fold}} = 19^{+4}_{-3}\,\mathrm{keV}$, $\Gamma = 1.46(8)$
`comptt`: $N_{\mathrm{H}} = 2.0^{+1.0}_{-0.8} \times 10^{22}\,\mathrm{cm}^{-2}$, $kT_0 = 1.0(1)\,\mathrm{keV}$, $A_{\mathrm{Fe}} = 1.0(3) \times 10^{-4}\,\mathrm{ph\,cm^{-2}\,s^{-1}}$,
$kT_{\mathrm{e}} = 5.6^{+0.7}_{-0.5}\,\mathrm{keV}$, $\tau = 4.4^{+0.3}_{-0.4}$

These results are qualitatively consistent with those found by Marcu et al. (2011) for the `comptt` model and with the exception of not requiring complex absorption or a soft excess also with those of Mattana et al. (2006) for `cutoffpl` and with Masetti et al. (2007) for `comptt`.

Chandra-HETG Lightcurve

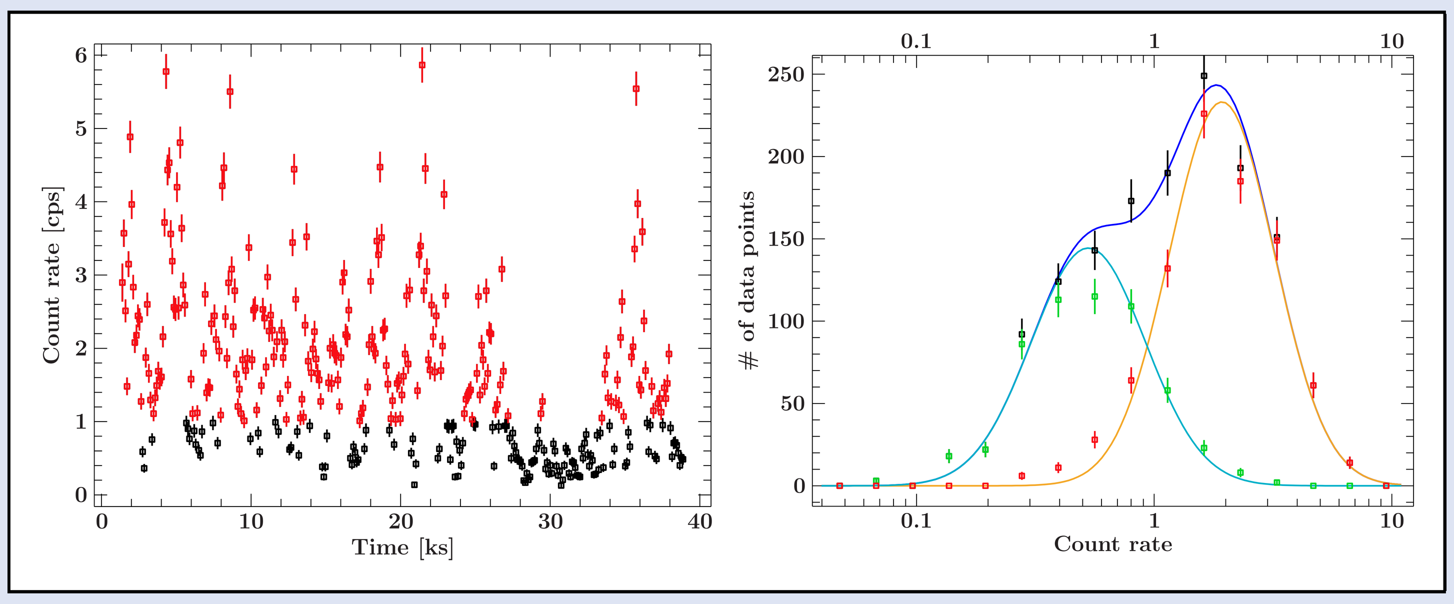

FIGURE 4: Left: Summed *Chandra* MEG & HEG 1st order 0.5–10 keV lightcurve with 104.4 s resolution. Flares with rates > 1 cps are marked in red. Right: Count rate distributions determined using 26.1 s bins (i) for the total lightcurve in black and (ii) for the time intervals defined by 104.4 bins with more and less than 1 cps, in red and green, respectively. The distribution of the overall logarithmic count rates can be described with two Gaussians which at the same time provide a good characterization of the flare and non-flare distributions (solid lines).

The summed MEG & HEG 1st order lightcurve over the total energy band spans two pulse cycles (Fig. 4, left). It shows strong flaring behavior, similar to the variability observed by Masetti et al. (2007) in lightcurves from *BeppoSax* and other instruments. Especially during the first pulse cycle this prevents the pulse from being visible, while the two main flares during the second pulse cycle are reminiscent of the double-peaked profile seen above 20 keV with *INTEGRAL* (Marcu et al., 2011).

The count rate distribution can be well described qualitatively by two log-normal components (Fig. 4, right). A similar study of the prototypical wind-accretor Vela X-1 by Fürst et al. (2010) has recently shown that its variability can be described by one log-normal component, which has been interpreted as a possible accretion shock signature of a clumpy wind.

RXTE-PCA Lightcurve

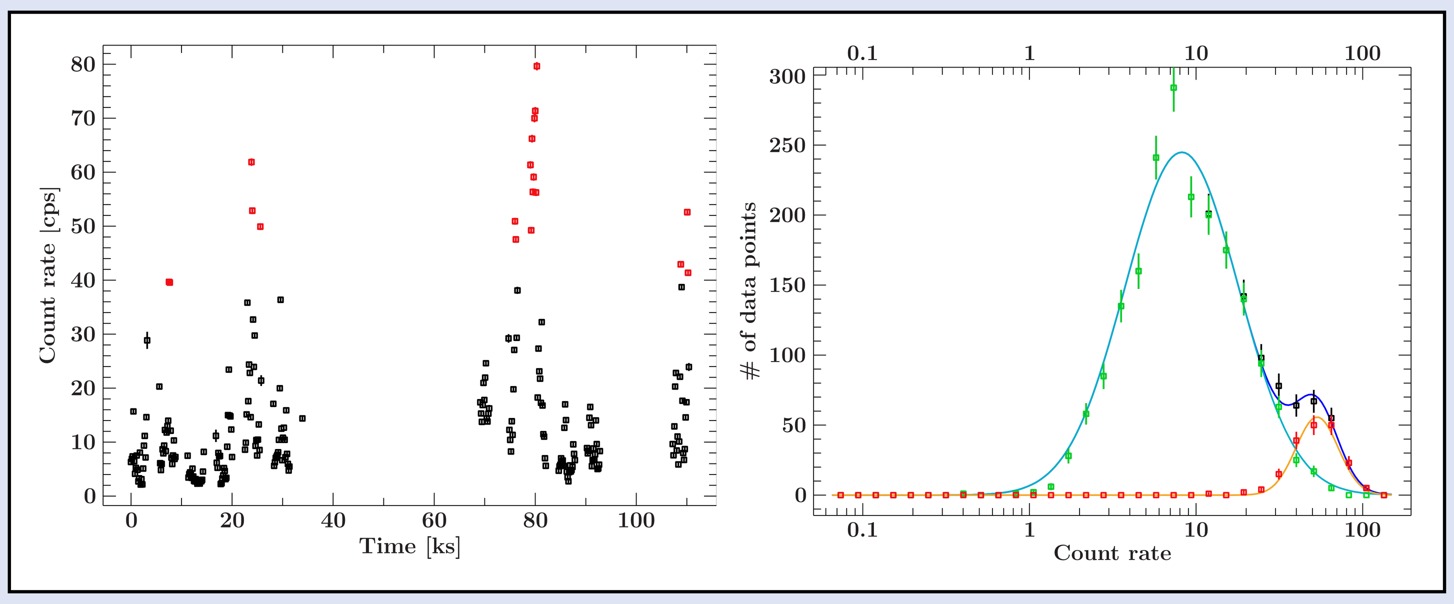

FIGURE 5: Left: Background-subtracted *RXTE* PCA PCU2 2–20 keV lightcurve with 160 s resolution. Flares with rates > 39 cps are marked in red. Right: Count rate distributions determined using 16 s bins (i) for the total lightcurve in black and (ii) for the time intervals defined by 160 bins with more and less than 1 cps, in red and green, respectively. The distribution of the overall logarithmic count rates can be described with two Gaussians which at the same time provide a good characterization of the flare and non-flare distributions (solid lines).

The PCA `standard2f` lightcurve over the total energy band spans 5.5 pulse cycles (Fig. 5, left). Like the *Chandra* lightcurve as well as like earlier observations (Masetti et al., 2007) it shows strong flaring. Again the pulse profile is not clearly visible, further complicated by the fact the total observation time corresponds to only two pulse cycles.

While the count rate distribution can be well described by two log-normal components in this case as well (Fig. 5, right), the ratio of flare to non-flare bins is very different. The ratio of the peak heights for *Chandra* is about 5/3, i.e., times of flaring dominate, whereas for *RXTE* it is about 1/5, i.e., times without flaring dominate. Future work has to show whether the two components observed for *Chandra* and *RXTE* correspond to each other and, if yes, whether their different ratios are due to different spectra or an evolution over time.

Summary

- The pulse period of 3A 1954+319 had slowed to ~5.8 h at ~MJD 56050 and is now spinning up again.
- Despite considerable variations in flux the X-ray continuum seems to be qualitatively unchanged. The absorbed 2–10 keV fluxes of the *Chandra*, *RXTE*, and 2008 *INTEGRAL* flare data are 2.23, 1.18, and 7.2 $\times 10^{-11}$ erg cm^{-2} s^{-1}, respectively.
- The *Chandra* HETG grating observation does not show any lines apart from Fe Kα emission.
- Both the *Chandra* and the *RXTE* count rate distributions can be described by two log-normal distributions, possibly indicating shocks in the wind release being accreted.

Outlook

- The next step will be to perform a joint fit of the *Chandra* HETG and *RXTE* PCA spectra.
- We also plan to model time resolved spectra following the criteria used to separate the two log-normals.
- The count rate distributions can be used to estimate the $\dot{M}_{\odot}$ distribution following Fürst et al. (2010).

References & Acknowledgments

Corbet R., Barbier L., Barthelmy S., et al., 2006, ATel 797
Corbet R.H.D., Sokoloski J.L., Mukai K., et al., 2008, ApJ 675, 1424
Forman W., Jones C., Cominsky L., et al., 1978, ApJS 38, 357
Fürst F., Kreykenbohm I., Pottschmidt K., et al., 2010, A&A 519, A37
Marcu D.M., Fürst F., Pottschmidt K., et al., 2011, ApJ 742, L11
Masetti N., Orlandini M., Palazzi E., et al., 2006, A&A 453, 295
Masetti N., Rigon E., Maiorano E., et al., 2007, A&A 464, 277
Mattana F., Götz D., Falanga M., et al., 2006, A&A 460, L1
Nespoli E., Fabregat J., Mennickent R.E., 2010, A&A 516, 94
Warwick R.S., Marshall N., Fraser G.W., et al., 1981, MNRAS 197, 865

KP and DMM acknowledge support from *Chandra* cycle 12 award No. GO1-12066A. In addition we thank the BMWi for support through DLR grants 50OR1107 (NH), 50OR0905 (SM), and 50OR1007 (VG). This research was also partly funded by LLNL under contract DE-AC52-07NA2734 (NH) and by the European Commission under grant agreement ITN 215212 "Black Hole Universe" (IM).